Integrating phase change material-based thermal energy storage with outdoor air systems for personalized wards

A conceptual framework

Su, Wei; Ai, Zhengtao; Yang, Bin; Du, Tiantian; Liu, Zhengxuan

DOI
10.1016/j.enbuild.2025.116875

Publication date
2026

Document Version
Final published version

Published in
Energy and Buildings

Citation (APA)
Su, W., Ai, Z., Yang, B., Du, T., & Liu, Z. (2026). Integrating phase change material-based thermal energy storage with outdoor air systems for personalized wards: A conceptual framework. *Energy and Buildings*, *352*, Article 116875. https://doi.org/10.1016/j.enbuild.2025.116875

Energy & Buildings 352 (2026) 116875

Contents lists available at ScienceDirect

Energy & Buildings

journal homepage: www.elsevier.com/locate/enb

Integrating phase change material-based thermal energy storage with outdoor air systems for personalized wards: A conceptual framework☆

Wei Su [a,b], Zhengtao Ai [a,b,*], Bin Yang [c], Tiantian Du [d], Zhengxuan Liu [e]

[a] Department of Building Environment and Energy, College of Civil Engineering, Hunan University, Changsha, China
[b] National Center for International Research Collaboration in Building Safety and Environment, Hunan University, Changsha, China
[c] School of Energy and Safety Engineering, Tianjin Chengjian University, Tianjin, China
[d] China Architecture Design & Research Group, Beijing, China
[e] Faculty of Architecture and the Built Environment, Delft University of Technology, Delft, Netherlands

ARTICLE INFO

Keywords:
Ward environment
Phase change material
Indoor air quality
Electricity savings

ABSTRACT

Creating an efficient ward environment is crucial for the sustainable development of healthcare buildings. This study proposes a methodological framework integrating a phase change material-based thermal energy storage outdoor air system (PCM-TES-OAS) to enable personalized ward environments, aiming to enhance patient comfort and respiratory health with low energy consumption. Four representative cities from different building climate zones in China, namely Beijing, Shenyang, Chengdu, and Shenzhen, were selected for a conceptual case study. The proposed system was theoretically evaluated against a conventional fan coil unit (FCU) plus dedicated OAS (FCU + DOAS) for its summer operational performance, indoor air quality impact, and energy-saving potential. The results indicate that the PCM-TES system remains operational for over 60 % of the time across all four cities. Moreover, the new system achieves an air change rate (ACH) of 8 h^{-1} to 10 h^{-1} while maintaining ward CO_2 concentrations consistently at a low level (below 500 ppm). In terms of energy performance, the total summer electricity savings are estimated to be no less than 60 kWh/m^2 in all evaluated cities. These theoretical findings demonstrate the system's conceptual potential to simultaneously improve patient comfort, enhance inhaled air quality, and reduce energy consumption in ward environmental control. Additionally, it is recommended that the maximum cooling capacity of the OAS and FCU in the new system be approximately 3 times and 0.3 times that of the conventional system, respectively. This study is anticipated to offer a conceptual framework and a promising new approach to designing comfortable, healthy, and sustainable ward environments.

1. Introduction

Creating an efficient ward environment is a fundamental aspect of sustainable healthcare architecture. It should exhibit three primary characteristics: (1) comfortable, (2) safe, and (3) sustainable. However, conventional air-conditioning systems face severe challenges such as low patient comfort level [1], high risk of cross-infection [2], and high energy consumption for environmental control [3], which pose significant threats to patients' physical and mental health, length of stay, and the sustainable development of hospital wards [4,5]. Personalized control of the bed micro-environment shows potential in addressing these issues simultaneously [6,7]. Furthermore, utilizing a phase change material-based thermal energy storage outdoor air system (PCM-TES-OAS) as the "source" for conditioning the bed micro-environment can not only further reduce air-conditioning energy consumption but also provide an integrated solution for system implementation.

For ward environmental control, existing guidelines generally recommend fan coil units (FCUs) coupled with dedicated outdoor air systems (DOAS), and the use of natural ventilation where feasible [8,9]. However, FCU + DOAS systems are designed to fully mix treated air with indoor air, failing to meet the diverse comfort needs of different patients. For instance, Zhen et al. [10] surveyed thermal satisfaction among 122 patients in a hospital in Xi'an, finding that over 70 % of patients felt too warm in summer and over 30 % reported significant discomfort. Moreover, in FCU + DOAS systems, OA may already be contaminated by the time it reaches the human breathing zone [11], creating substantial cross-infection risks during outbreaks. Additionally, since such systems aim to control the entire room space, they result in considerable energy waste in settings like wards that require 24-hour

☆ This article is part of a special issue entitled: 'ENB_Low-Carbon Comfort-Centric Buildings' published in Energy & Buildings.

* Corresponding author at: Department of Building Environment and Energy, College of Civil Engineering, Hunan University, Changsha, China.
E-mail address: zhengtaoai@hnu.edu.cn (Z. Ai).

https://doi.org/10.1016/j.enbuild.2025.116875
Received 17 September 2025; Received in revised form 6 December 2025; Accepted 12 December 2025
Available online 13 December 2025

Nomenclature

C_P	Specific heat capacity, kJ/(kg·K)
C_{supply}	CO_2 concentration of outdoor air, ppm
C_{ward}	Average CO_2 concentration of ward, ppm
$C_{ward,i}$	Average CO_2 concentration of ward at moment i, ppm
$C_{ward,i+\Delta t}$	Average CO_2 concentration of ward at moment $i+\Delta t$, ppm
e	Correction factor
$E_{c-total}$	Total system power consumption, kWh
G_r	Total CO_2 release rate, ml/s
H	Human height, m
m	Mass flow rate, kg/s
M	Metabolic rate, W/m^2
q_{fresh}	Airflow rate of outdoor air, m^3/s
Q_{coil}	Cooling load handled by fan coil unit, kW
Q_{c-coil}	Required cooling capacity of fan coil unit, kW
$Q_{c-fresh}$	Required cooling capacity of outdoor air system, kW
Q_{CO_2}	CO_2 release rate, ml/s
Q_{ec}	Hourly energy change, kJ
Q_r	Remaining cooling load, kW
Q_{st-i}	Available cool storage at moment i, kJ
$Q_{st-i-\Delta t}$	Available cool storage at moment $i-\Delta t$, kJ
Q_T	Cooling load removed by bed terminal, kW
Q_{ward}	Total cooling load of ward, kW
$T_{outdoor}$	Outdoor air temperature, K
T_{outlet}	Outlet air temperature, K
T_{set}	Ward set-point temperature, K
T_{supply}	Supply air temperature, K
V	Ward volume, m^3
W	Human mass, kg
ρ	Density, kg/m^3
ACH	Air changes per hour
DOAS	Dedicated outdoor air system
HVAC	Heating, ventilation, and air conditioning
PCM	Phase change material
PECS	Personal environmental control system
PV	Personalized ventilation
RQ	Respiratory quotient
TES	Thermal energy storage

conditioning [12]. While natural ventilation can partially mitigate these problems [13], its effectiveness is highly dependent on outdoor weather conditions and is often unstable [14,15].

Personalized environmental control systems (PECS), such as various personalized ventilation (PV) systems [16] and local radiant systems [17], have demonstrated the ability to reduce cross-infection risk and effectively improve occupant comfort levels. The value and implementation frameworks of PECS are gaining broader recognition, as highlighted in recent international collaborative research and review papers [18]. For example, Su et al. [11] compared five common air distribution patterns and found that PV systems resulted in the lowest cross-infection risk. Experimental results from Melikov et al. [19] showed that local cooling radiant panels effectively improved thermal comfort and perceived air quality. However, most existing PECS are designed for office environments. For bedridden patients, currently proposed systems remain limited, primarily including ventilated mattresses and local exhaust devices near the bedhead. For instance, Bivolarova et al. [6,20,21] systematically evaluated the performance of ventilated mattresses, finding they can effectively reduce patient exposure to biological and airborne contaminants while improving thermal comfort. Su et al. [22] demonstrated that installing local exhaust devices at the bedhead significantly reduced patient exposure to gaseous and particulate pollutants, thereby improving inhaled air quality. Nevertheless, existing devices have two main limitations: (1) Regarding the devices themselves, the performance of ventilated mattresses has not been thoroughly evaluated – issues include limited adaptability to body posture changes, inconsistent exhaust performance, and potential local discomfort [23]. Local exhaust devices, on the other hand, often have limited effectiveness in improving comfort [22]; (2) Existing research on PECS in wards predominantly focuses on the interaction between the patient and the terminal device, with little in-depth exploration of how these terminals integrate and cooperate with existing HVAC systems. This gap in systemic integration, which is crucial for practical application, is also identified as a key challenge in the wider PECS literature [24]. To address these gaps, we previously proposed a novel terminal device for bed micro-environment control and performed multi-objective optimization of its design parameters. This device aims to deliver OA directly to the bed area, simultaneously fulfilling patient comfort needs, respiratory health requirements, and energy-saving goals in wards [25,26]. Similarly, the design of the "source" system for this novel terminal remains unresolved.

PCM-TES technology has been widely applied in building energy efficiency. For instance, numerous studies have integrated PCMs with photovoltaics [27,28] and building envelopes [29–31], and their energy-saving potential is well examined. Regarding the integration of PCMs with HVAC systems, combining PCMs with OAS is one of the most common approaches [32–34], also known as the PCM-TES-OAS. The primary purpose of a PCM-TES-OAS is to pre-condition outdoor OA before it enters the air handling unit, thereby reducing the energy consumption of the unit. As early as 2004, Takeda et al. [35] simulated the application potential of PCM-TES-OAS, showing that such systems could reduce ventilation load by up to 62.8 %, with performance highly dependent on fluctuations in outdoor temperature. Masood et al. [32] experimentally and numerically evaluated the performance of a PCM-TES-OAS under extreme heat conditions, demonstrating its ability to pre-cool OA from 46 ℃ to 33 ℃ before it enters the air handling unit. Moreover, using PCM-TES-OAS significantly improved the efficiency of the air-conditioning system, particularly during peak load periods. Palanisamy and Ayalur [36] investigated the impact of PCM-TES-OAS on indoor air quality, finding it effective in reducing indoor CO_2 concentrations. Current research increasingly focuses on enhancing the heat transfer efficiency between PCM storage units and heat transfer fluids to improve system performance [37–39]. Meanwhile, many researchers are dedicated to developing corresponding performance prediction models and design frameworks [40,41]. However, similar to research on PECS, current studies on PCM-TES-OAS largely concentrate on the systems themselves, with research on their coupling with indoor environments still scarce.

Considering the characteristics of both PECS and PCM-TES-OAS, integrating PCM-TES-OAS with PECS in wards can provide a comprehensive solution for enhancing patient satisfaction, reducing cross-infection risks, and lowering ward energy consumption. For PECS, this integration addresses the need for a suitable "source" and further reduces environmental control energy use. For PCM-TES-OAS, it enhances the utilization efficiency of OA and safeguards patients' respiratory health. Therefore, this study aims to investigate the performance of a PCM-TES-OAS in personalized ward environmental control, including its systemic performance, impact on indoor air quality, and energy-saving potential. This research is expected to offer a new technological pathway for creating comfortable, healthy, and sustainable ward environments.

2. Methods

2.1. Introduction of the newly developed system

This study will use the traditional FCU + DOAS system as a baseline to introduce specific improvements implemented in the new system. Meanwhile, this study will focus on the summer condition. A schematic diagram comparing the FCU + DOAS system and the proposed new system is presented in Fig. 1.

In the traditional FCU + DOAS system (Fig. 1 (a)), the indoor set-point temperature is typically set at 24 ℃ [8,9]. The OAS is usually designed to supply OA at a rate of 2 air changes per hour (ACH). Both OA and indoor return air are generally supplied into the ward through diffusers located near the ceiling [42].

In the new system, OA is conditioned by the PCM-TES-OAS and delivered directly to each patient bed by the specifically designed terminal [25,26]. The designed maximum OA flow rate for each bed is initially set at 50 L/s, a value slightly higher than the optimum identified in previous studies [25]. This adjustment accounts for individual demand variations in real-world scenarios. Furthermore, patients can freely adjust the airflow rate via a flow control valve, with any excess conditioned OA being supplied to other areas of the ward. The designed supply air temperature of the PCM-TES-OAS and FCU is considered as 22 ℃. This fixed setpoint is maintained to ensure a stable air supply rate for consistent indoor air quality assessment, and to provide a reliable cooling source for the personalized terminal across the investigated range of room set-point temperatures (24–28 ℃).

When the bed micro-environment is independently controlled by the PCM-TES-OAS, the ward set-point temperature can be appropriately elevated. For this study, the set-point temperature is set at 28 ℃, the feasibility of which has been demonstrated in prior research [25].

The specific operational strategy of the PCM-TES system is illustrated in Fig. 2. First, for a given PCM-TES system and operating flow rate, the outlet air temperature of the PCM-TES can be determined based on the dry-bulb temperature of the OA. A decision is then made by comparing this outlet temperature with the OA temperature to determine whether the DOAS should handle the OA directly or the air that has passed through the PCM-TES. If the DOAS is to handle OA directly, the relationship between the OA temperature and the PCM temperature is evaluated:

If the OA temperature is higher than the PCM temperature, the PCM-TES is deactivated.
If the OA temperature is lower than the PCM temperature, the PCM-TES is activated to store cooling energy.

If the DOAS is to handle the air preconditioned by the PCM-TES, the PCM-TES remains active to continuously precondition the OA.

2.2. Case study setup

2.2.1. Information of the ward

This study will focus on the regions of Beijing, Shenyang, Chengdu, and Shenzhen, which represent China's cold climate zone, severe cold climate zone, hot summer and cold winter climate zone, and hot summer and warm winter climate zone, respectively. The temperate climate zone, including cities such as Kunming, is not considered in this study due to its generally low ventilation load. The detailed geometrical information of the ward is illustrated in Fig. 3. In this study, a double-occupancy ward with dimensions of 8 m × 5 m × 3 m (length × width × height) is used as the case study. With these dimensions, the spacing between patient beds complies with relevant design standards [8]. To better reflect real-world conditions, the ward is considered to have one external wall, with a window-to-wall ratio set at 0.5 [43].

The building envelope parameters of the ward are presented in Table 1. It is noteworthy that heat transfer through the internal wall, floor, and ceiling is neglected in this study, as it is typically minimal under actual conditions. Furthermore, the focus of this research is not on analyzing heat gain within the ward, but rather on evaluating the impact of the new system on the ward's environmental conditioning. In addition, the internal heat sources included three occupants (120 W/person), lighting (13 W/m^2), and equipment (1600 W).

2.2.2. Operating conditions

This study considers system operation during the three summer months (June, July, and August). For both the conventional FCU + DOAS and the new system, the specific design parameters are consistent with those shown in Fig. 1. It is noteworthy that for the FCU system, the supply air temperature under both operating modes is maintained at 22 ℃, consistent with that of the PECS. Furthermore, regardless of the cooling load conditions within the ward, the minimum OA volume remains constant for both systems.

2.2.3. Design of the PCM-TES system

The performance of the PCM-TES system significantly influences the overall operational state of the new system. However, this study does not aim to identify the currently best-performing PCM-TES for investigation. This is because existing research continuously optimizes and enhances the performance of PCM-TES systems [44,45]. Therefore, a commonly used and widely recognized plate-type PCM-TES unit with well-established performance is selected as a representative case for this study [46]. Regarding the PCM selection, paraffin wax-a material frequently adopted in related studies is chosen. Detailed information regarding the PCM-TES is presented in Fig. 4. Regarding the phase change temperature, seven values are considered: 18 ℃, 20 ℃, 22 ℃, 24 ℃, 26 ℃, 28 ℃, and 30 ℃. These temperatures are commonly used in studies related to heat exchange between PCM and OA [47].

The performance parameters of the designed PCM-TES system, predicted using our previously developed model under various operating

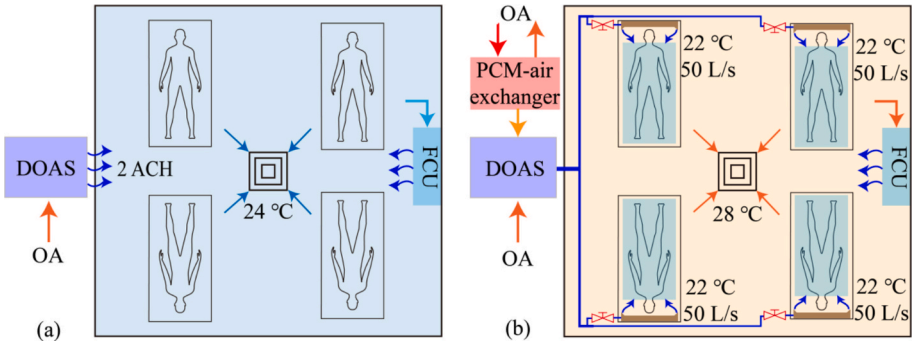

Fig. 1. (a) The traditional FCU + DOAS system. (b) The newly developed system.

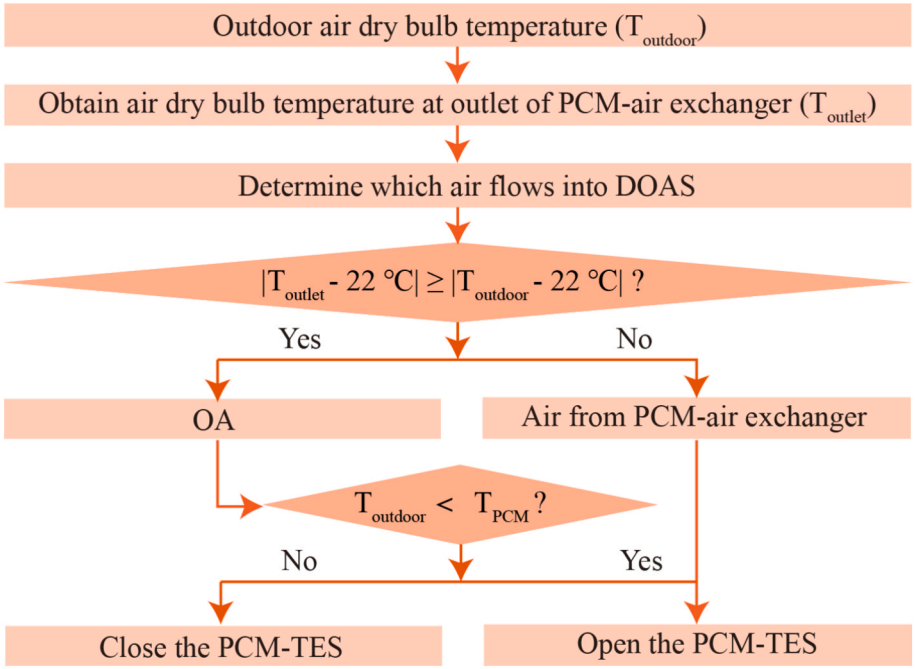

Fig. 2. Method for determining the operating status of the PCM-TES-OAS.

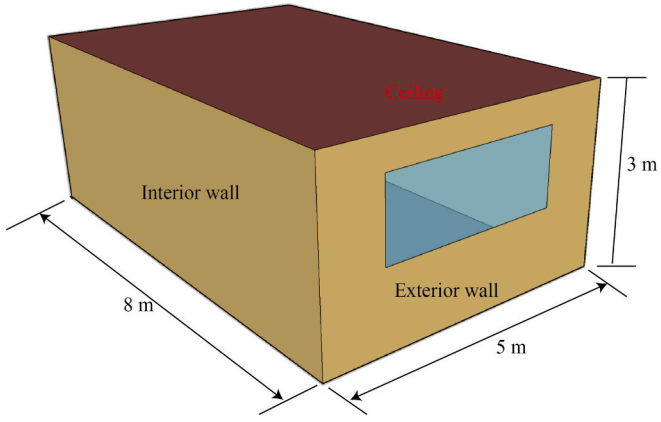

Fig. 3. Geometry of the ward.

Table 1
Parameters of the ward's envelope.

Parameters	Beijing	Shenyang	Chengdu	Shenzhen
Heat transfer coefficient of the exterior wall, W/(m^2·K)	0.45	0.35	0.6	0.8
Heat transfer coefficient of the window, W/(m^2·K)	1.9	1.7	2.4	2.7
Solar heat gain coefficient	0.43	/	0.35	0.28
Thickness of the exterior wall, cm	37	45	24	24

conditions [40], are summarized in Table 2. The system demonstrates the capability to operate effectively for 12 h under an outdoor temperature of 38 °C and an inlet airflow rate of 50 L/s. As illustrated in Fig. 4 (a), each PCM-TES unit is designed to serve a single bed terminal. The flow rate during the charging mode is configured at three times that of the discharging mode [48], corresponding to a value of 150 L/s.

2.3. Performance evaluation method

2.3.1. Evaluation of PCM-TES system's operating status

In this study, the operational status of the PCM-TES system is primarily evaluated based on its uptime percentage throughout the three summer months, its hourly on/off status, and the hourly fluctuation of its available cool storage. Both the uptime percentage and the hourly on/off status can be determined using the operational decision-making flowchart presented in Fig. 2. To obtain the hourly variation in available cool storage, the hourly energy change of the PCM-TES system should be calculated in advance:

$$Q_{ec} = 3600 * C_p * m * (T_{outdoor} - T_{outlet}) \quad (1)$$

where Q_{ec} is the hourly energy change of the PCM-TES system, kJ; C_p is the specific heat capacity of the air, kJ/(kg·K); m is the mass flow rate of the PCM-TES system, kg/s.

Then, the available cool storage at the moment i can be determined:

$$Q_{st-i} = Q_{st-i-\Delta t} + Q_{ec} \quad (2)$$

Where $Q_{st-i-\Delta t}$ is the available cool storage at the moment $i-\Delta t$, kJ; Δt is the time interval (3600 s). It is noteworthy that Q_{st-i} always satisfies $0 \leq Q_{st-i} \leq Q_{st-max}$, where Q_{st-max} denotes the maximum cooling storage capacity of the PCM-TES system.

2.3.2. Evaluation of indoor air quality

The commonly used CO_2 concentration will be considered as the indoor pollutant of the ward [49]. The hourly variation of CO_2 concentration in the ward and its average value over the three-month period are be used to assess the indoor air quality level. In the ward, the CO_2 is produced by persons, and the CO_2 release rate of each person can be calculated by the following equation:

$$Q_{CO_2} = e \cdot \frac{0.202RQ \cdot M \cdot H^{0.725} \cdot W^{0.425}}{21(0.23RQ + 0.77)} \quad (3)$$

where e is the correction factors for Chinese males and females (0.85 for males and 0.75 for females) [50]; RQ is the respiratory quotient (0.83) [51]; M is the metabolic rate of patients, W/m^2; H is the human height,

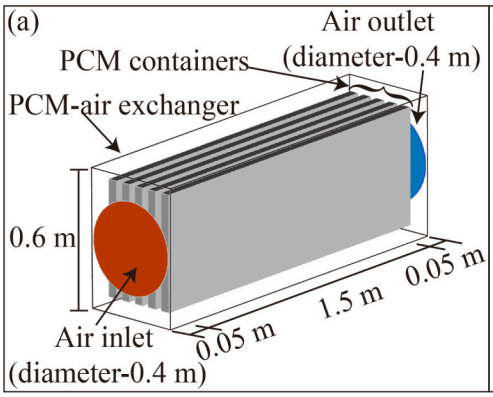

(c)

Properties	Paraffin-A series products
Specific heat capacity	2 kJ·(kg·K)$^{-1}$
Thermal conductivity	0.2 W·(m·K)$^{-1}$
Density	800 kg·m^{-3}
Latent heat	210 kJ·kg^{-1}

Fig. 4. (a) Overall view of the PCM-TES. (b) Side view of the PCM-TES. Thermophysical parameters of the selected PCM.

Table 2
Functional relationship between the inlet and outlet temperature of the PCM-TES.

Types of PCM	Discharging mode (50 L/s)	Charging mode (150 L/s)	R^2
Paraffin A-18	$T_{out} = 0.52T_{in} + 8.6$	$T_{out} = 0.68T_{in} + 5.9$	0.99
Paraffin A-20	$T_{out} = 0.53T_{in} + 9.4$	$T_{out} = 0.68T_{in} + 6.4$	
Paraffin A-22	$T_{out} = 0.53T_{in} + 10.3$	$T_{out} = 0.68T_{in} + 7.1$	
Paraffin A-24	$T_{out} = 0.53T_{in} + 11.3$	$T_{out} = 0.68T_{in} + 7.7$	
Paraffin A-26	$T_{out} = 0.53T_{in} + 12.2$	$T_{out} = 0.68T_{in} + 8.3$	
Paraffin A-28	$T_{out} = 0.53T_{in} + 13.2$	$T_{out} = 0.68T_{in} + 8.9$	
Paraffin A-30	$T_{out} = 0.53T_{in} + 14.2$	$T_{out} = 0.68T_{in} + 9.4$	

m; W is the human mass, kg.

Assuming that CO_2 is uniformly distributed within the ward, the variation in average CO_2 concentration can be derived based on the mass conservation relationship:

$$V\frac{dC_{ward}}{dt} = q_{fresh}\cdot(C_{supply} - C_{ward}) + G_r \tag{4}$$

where V is the volume of the ward, m^3; C_{ward} is the average CO_2 concentration within the ward, ppm; q_{fresh} is the airflow rate of OA, m^3/s; C_{supply} is the CO_2 concentration of OA, ppm; G_r is the total CO_2 release rate, ml/s.

Adopting t as a time interval, the evolution of time-varying CO_2 concentration can be obtained using the discrete scheme of the differential Eq. (4).

$$C_{ward,i+\Delta t} = \frac{G_r}{V}\cdot\Delta t - ACH\cdot\Delta t\cdot(C_{ward,i} - C_{supply}) + C_{ward,i} \tag{5}$$

where $C_{ward,i}$ and $C_{ward,i+\Delta t}$ are the average ward CO_2 concentration at moment i and $i + \Delta t$, respectively.

In this way, the evolution of average ward CO_2 concentration throughout the three summer months can be calculated using the Eq. (5). Finally, this study considers two scenarios: one with four people (two males and two females) and the other with eight people (four males and four females) in the ward. The C_{supply} is considered as 400 ppm [51].

2.3.3. Evaluation of electricity savings

In this study, the total system power consumption will be used to evaluate the energy-saving potential of the new system. Prior to calculating power consumption, the total cooling capacity provided by the system must be determined (see Fig. 5).

Firstly, the airflow rate handled by the OAS must be determined based on the operating status of the PCM-TES system. When the PCM-TES system is deactivated, or when it is activated and operating in discharging mode, the airflow rate is 0.2 m^3/s (serving four terminals, each at 0.05 m^3/s). When the PCM-TES is active and in charging mode, if the air passing through it is exhausted directly outdoors (see Fig. 2), the airflow rate remains 0.2 m^3/s. If the air exiting the PCM-TES can be directly introduced into the OAS, the remaining cooling load within the room must be determined first.

$$Q_r = Q_{ward} - Q_T \tag{6}$$

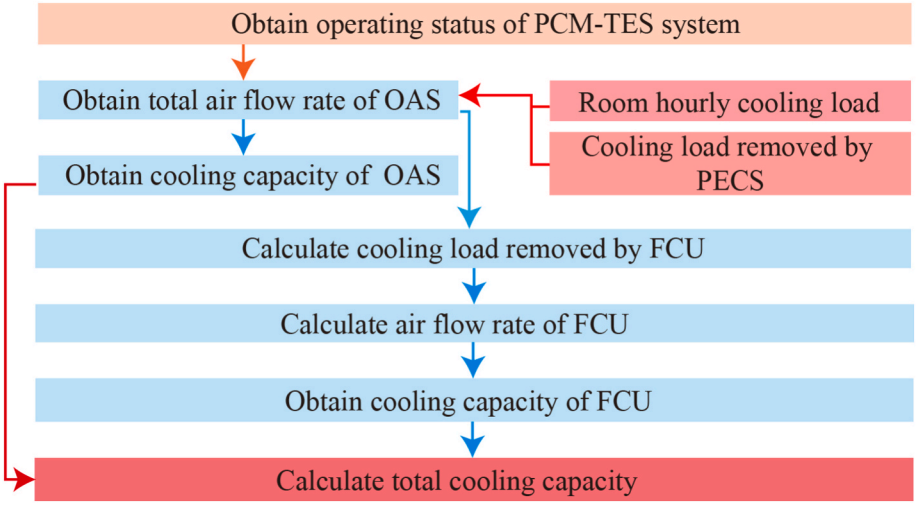

Fig. 5. Flowchart for calculating the total cooling capacity required by the system.

$$Q_T = 0.2C_P\rho(T_{set} - T_{supply}) \tag{7}$$

where Q_r is the remaining cooling load in the ward, kW; Q_{ward} is the total cooling load in the ward, kW; Q_T is the cooling load removed by the bed terminal, kW; T_{set} is the ward set-point temperature, K; T_{supply} is the air supply temperature of the bed terminal, K.

Since the PCM-TES system operates at triple the flow rate in charging mode, the additional airflow capacity beyond the predetermined 0.05 m^3/s per bed terminal can be utilized to handle a portion of the ward's cooling load. The corresponding cooling capacity is given by:

$$Q_D = 2Q_T \tag{8}$$

At this time, if $Q_r \geq Q_D$, the total airflow rate of the OAS (q_{fresh}) is 0.06 m^3/s. Otherwise, it is calculated using the following equation:

$$q_{fresh} = \frac{Q_r}{C_P\rho(T_{set} - T_{supply})} + 0.2 \tag{9}$$

Once the q_{fresh} is determined, the required cooling capacity of the OAS must be calculated. When the PCM-TES system is active and its outlet air is directly supplied to the OAS, the required cooling capacity ($Q_{c-fresh}$) is given by:

$$Q_{c-fresh} = C_P\rho q_{fresh}\left|T_{outdoor} - T_{supply}\right| \tag{10}$$

Meanwhile, the cooling load to be handled by the FCU (Q_{coil}) can be calculated as follows:

$$Q_{coil} = Q_{ward} - C_P\rho q_{fresh}(T_{set} - T_{supply}) \tag{11}$$

Then, the airflow rate of the FCU (q_{coil}) can be determined:

$$q_{coil} = \frac{Q_{coil}}{C_P\rho(T_{set} - T_{supply})} \tag{12}$$

In this way, the required cooling capacity of FCU (Q_{c-coil}) can be obtained:

$$Q_{c-coil} = C_P\rho q_{coil}\left(T_{set} - T_{supply}\right) \tag{13}$$

Finally, the total system power consumption can be calculated using the following equation:

$$E_{c-total} = \frac{t\left(Q_{c-fresh} + Q_{c-coil}\right)}{EER} \tag{14}$$

where $E_{c-total}$ is the total system power consumption, kWh; t is the running duration, h; EER is the energy efficiency ratio of the air conditioning system, taken as 3.0 [52].

2.4. Simulation process

Regarding the specific simulation process, typical meteorological year data for the four cities, obtained from the official EnergyPlus website, were first utilized as input. The hourly cooling loads of the ward over the three summer months for each city were then calculated based on the ward's physical information and internal heat sources provided in Section 2.2.1. Simultaneously, the outlet air temperature of the PCM-TES at each time step was determined using its heat exchange effectiveness listed in Table 2. The operational status of both the PCM-TES and the OAS was subsequently determined according to the control logic outlined in Fig. 2. Following this, the operation of the ward's FCU was defined based on the calculated hourly cooling load, as described in Section 2.3.3.

For the indoor air quality assessment, once the system's operational state was determined, the flow rate of OA entering the ward was known. The hourly CO_2 concentration in the ward could then be solved using the method detailed in Section 2.3.2. Consequently, given the predetermined outdoor weather parameters, PCM-TES performance, bed terminal operation, ward's setpoint temperature, and the system's control logic, the output results – including system operational status, indoor CO_2 concentration, and electricity savings – were unique. In this study, the implementation of the system's control logic and the derivation of all output results were achieved through programming in MATLAB (Version R2022a).

2.5. Model validation and assumptions

To ensure the robustness and replicability of the findings, this study employs a hybrid simulation approach, the core principles and limitations of which are detailed herein.

The validation of the integrated model is conducted in several ways. First, the heat transfer effectiveness of the PCM-TES unit, a critical model input, is not an arbitrary assumption but is based on the experimentally validated mathematical model [40]. Second, the custom operational control logic and the indoor CO_2 concentration algorithm, implemented in MATLAB, are verified for logical consistency. This verification involves running the model under a series of predefined boundary conditions (e.g., extremely high and low outdoor temperatures) and confirming that the system's operational state switches and concentration outputs align with theoretical expectations. Finally, the reasonableness of the hourly building cooling load calculated by EnergyPlus is cross-checked against results from a simplified manual calculation based on the ASHRAE heat balance method, confirming that the baseline load falls within a credible range.

The simulation framework relies on several key assumptions necessary to define the scope of this initial investigation:

(1) The indoor air is assumed to be perfectly mixed for the purpose of calculating the average CO_2 concentration.
(2) The Energy Efficiency Ratio (EER) of the central chiller plant is held constant at a value of 3.0 for the electricity consumption calculation.
(3) Internal heat gains from occupants, lighting, and medical equipment are treated as constant values of 120 W/person, 13 W/m^2, and 1600 W, respectively.
(4) The supply air temperature for both the FCU and the PCM-TES-OAS is maintained at a constant 22 ℃ to ensure stable performance of the personalized terminal and a consistent basis for comparing system performance.
(5) The charge and discharge processes of the PCM are modeled using a fixed effectiveness, and transient effects such as hysteresis are not considered.

3. Results

3.1. Operating status of the PCM-TES system

3.1.1. Uptime percentage of the system

Fig. 6 shows the uptime percentage of the PCM-TES system when using different types of PCM. In Beijing, as the phase change temperature increased from 18 ℃ to 26 ℃, the system's uptime percentage during the three summer months rose from 4 % to 75 % (the maximum value). However, when the phase change temperature continued to increase, the uptime percentage gradually decreased. At a phase change temperature of 30 ℃, the uptime percentage dropped to only 30 %.

In Shenyang, Chengdu, and Shenzhen, the relationship between uptime percentage and phase change temperature was similar to that in Beijing: as the phase change temperature increased, the uptime percentage first increased and then decreased. The maximum uptime percentages of the PCM-TES system in Shenyang, Chengdu, and Shenzhen were 61 %, 74 %, and 76 %, respectively. These maxima occurred at phase change temperatures of 24 ℃, 24 ℃, and 28 ℃, respectively. These results indicated that by selecting an appropriate PCM, the PCM-TES system could remain operational for most of the summer in all four cities.

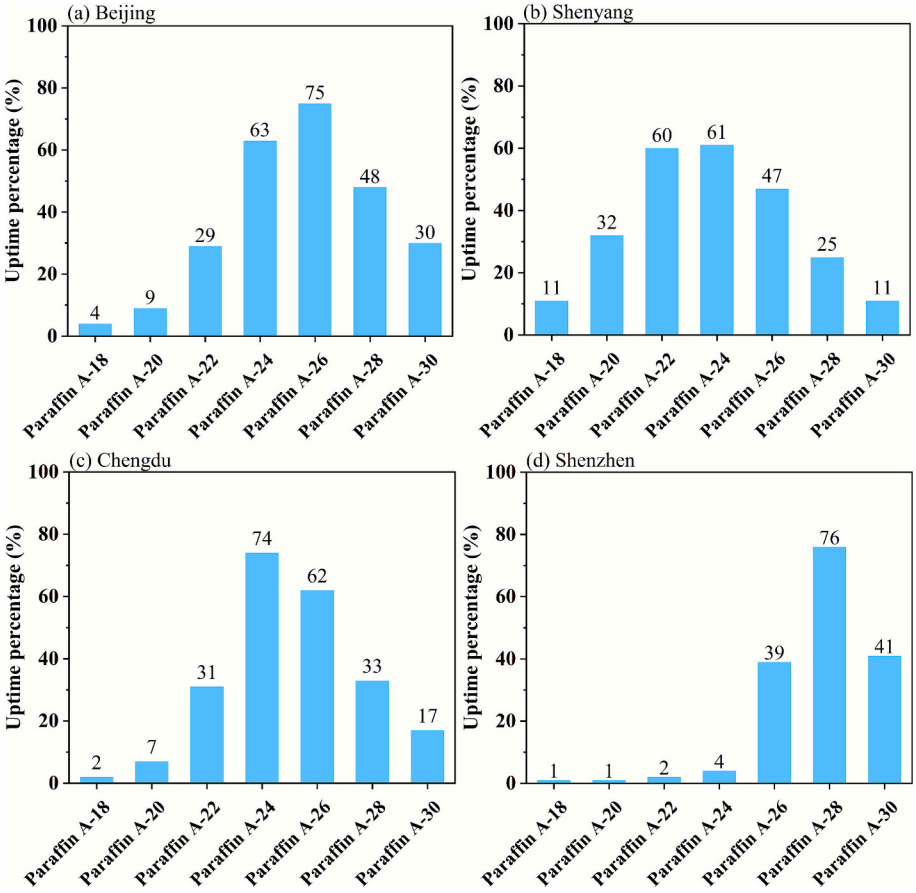

Fig. 6. Uptime percentage of the PCM-TES system under different phase change temperatures for the three summer months. (a) Beijing. (b) Shenyang. (c) Chengdu. (d) Shenzhen.

3.1.2. *Hourly on/off status of the system*

The hourly on/off status of the PCM-TES system during summer in the four cities is shown in Fig. 7. It should be noted that only the case with the maximum uptime percentage was displayed, as scenarios involving other phase change temperatures were not further investigated in this study since they did not represent the optimal choice.

In Beijing, the PCM-TES system remained mostly deactivated in early June but operated nearly continuously from June 15 to July 31. Throughout August, the system exhibited frequent switching between on and off states. Compared to Beijing, the period of sustained operation in Shenyang was relatively shorter, concentrated mainly between June 30 and July 15. During other periods, the system switched on and off more frequently. In Chengdu, the system operated continuously for extended periods between June 15 and July 15, and again from August 15 to the end of August. In Shenzhen, the system ran continuously from mid-June to early July. Although more frequent cycling occurred during other time intervals, the system remained operational most of the time. Overall, the operational durations shown in Fig. 7 were consistent with the specific numerical values presented in Fig. 6.

3.1.3. *Available cool storage*

The hourly available cool storage of the PCM-TES system during summer is shown in Fig. 8. Consistent with Section 3.1.2, only the case with the maximum uptime percentage was considered in Fig. 8. Additionally, the maximum value of available cool storage in the figure corresponded to the full latent heat storage capacity of the system, i.e., 100.8 MJ.

In Beijing, it could be observed that the available cool storage of the PCM-TES system barely changed in early June. Starting from mid-June, the available cool storage exhibited hourly fluctuations. Around July 31, the system's available cool storage decreased continuously until it reached 0 MJ. However, this condition did not persist as it recovered to around 100 MJ in early August and continued to fluctuate within a narrow range until the end of the month.

In Shenyang, the available cool storage of the PCM-TES system showed minor fluctuations throughout June, remaining between 80 MJ and 100 MJ. During July, however, the available cool storage varied widely, with values frequently bottoming out for extended periods in mid-to-late July. It was not until early August that the available cool storage gradually recovered to its maximum level. Throughout the rest of August (mid- and late August), the system's available cool storage fluctuated only within a small range.

Compared with Shenyang, the PCM-TES system in Chengdu experienced longer periods during which the available cool storage remained at the minimum value (0 MJ). This was particularly evident from mid-July to mid-August, when the available cool storage stayed at 0 MJ for prolonged durations. In addition, the available cool storage repeatedly dropped to the minimum value in mid-June and early July. Although it did not reach minimum levels during other periods, the amplitude of fluctuation was still significantly greater than that in Beijing and Shenzhen.

In Shenzhen, the available cool storage of the PCM-TES system began to show substantial fluctuations from mid-June, accompanied by an overall declining trend. By early July, the available cool storage gradually decreased to 0 MJ. However, this condition was short-lived. By around July 15, it had recovered to the maximum value. During the latter half of the summer, the available cool storage fluctuated only within a relatively narrow range of 60 MJ to 100 MJ.

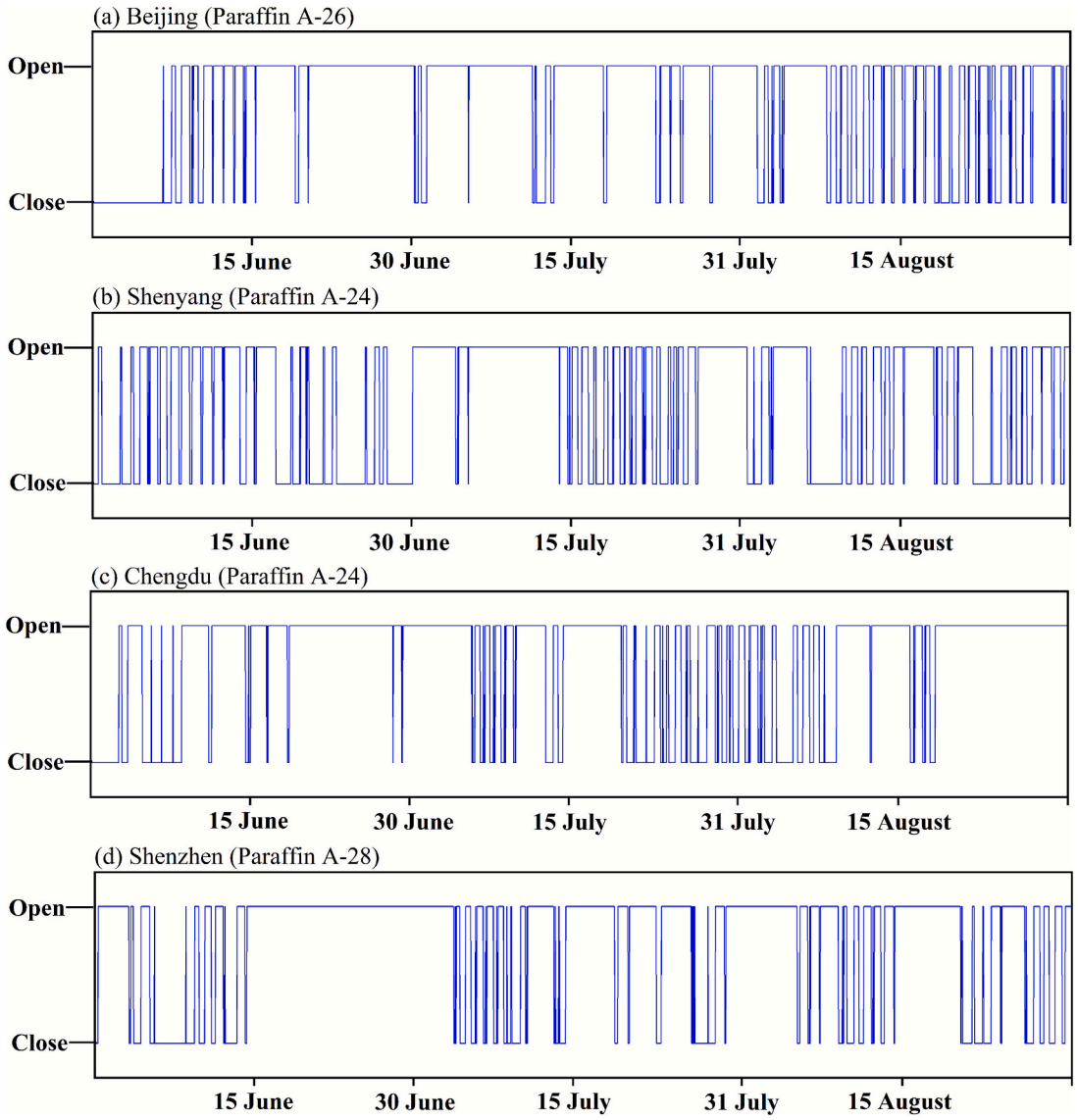

Fig. 7. Hourly on/off status of the PCM-TES system across the summer months, shown for the optimal PCM type (maximum uptime). (a) Beijing. (b) Shenyang. (c) Chengdu. (d) Shenzhen.

3.2. Air quality in the ward

When the total number of people in the ward was four (two males and two females), the evolution of average CO_2 concentration is shown in Fig. 9. The blue line represented the CO_2 concentration under the new system, while the red line denoted that under the conventional system (with an ACH of 2 h^{-1}). Prior to the start of ventilation, the average CO_2 concentration in the ward was 450 ppm.

As shown in Fig. 9, when the ward was conditioned by the conventional system, the average CO_2 concentration remained consistently around 550 ppm. In contrast, when the new system was employed, the average CO_2 decreased significantly across all four cities. The average concentrations during the three summer months in Beijing, Shenyang, Chengdu, and Shenzhen were 437 ppm, 433 ppm, 434 ppm, and 434 ppm, respectively. Moreover, in all four cities, the average CO_2 concentration fluctuated only between 420 ppm and 450 ppm throughout the summer.

When the total number of people increased to eight (four males and four females), the variation in average CO_2 concentration is presented in Fig. 10. It could be observed that when the conventional system was used, the average CO_2 concentration remained consistently at 700 ppm. When the new system was applied, the hourly variation trend of the average CO_2 concentration was identical to that under the four-people scenario (refer to Fig. 9). However, the overall concentration level was higher than that in Fig. 9. The summer average CO_2 concentrations in Beijing, Shenyang, Chengdu, and Shenzhen increased to 473 ppm, 467 ppm, 468 ppm, and 468 ppm, respectively. Additionally, the fluctuation range of the average concentration also increased, varying between 440 ppm and 500 ppm across all four cities during summer.

Finally, Figs. 9 and 10 demonstrate that even when occupant density increased from 10 m^2/person to 5 m^2/person, the CO_2 concentration in the ward controlled by the new system remained at a relatively low level. Furthermore, compared to the conventional system, the new system resulted in significantly lower CO_2 concentrations in the ward. For the average ACH throughout the three summer months, it reached by 8.7 h^{-1}, 9.4 h^{-1}, 9.1 h^{-1}, and 9.3 h^{-1} for Beijing, Shenyang, Chengdu, and Shenzhen, respectively.

3.3. Electricity savings

The total summer electricity savings of the new system compared to the conventional system, using different types of PCM, are shown in

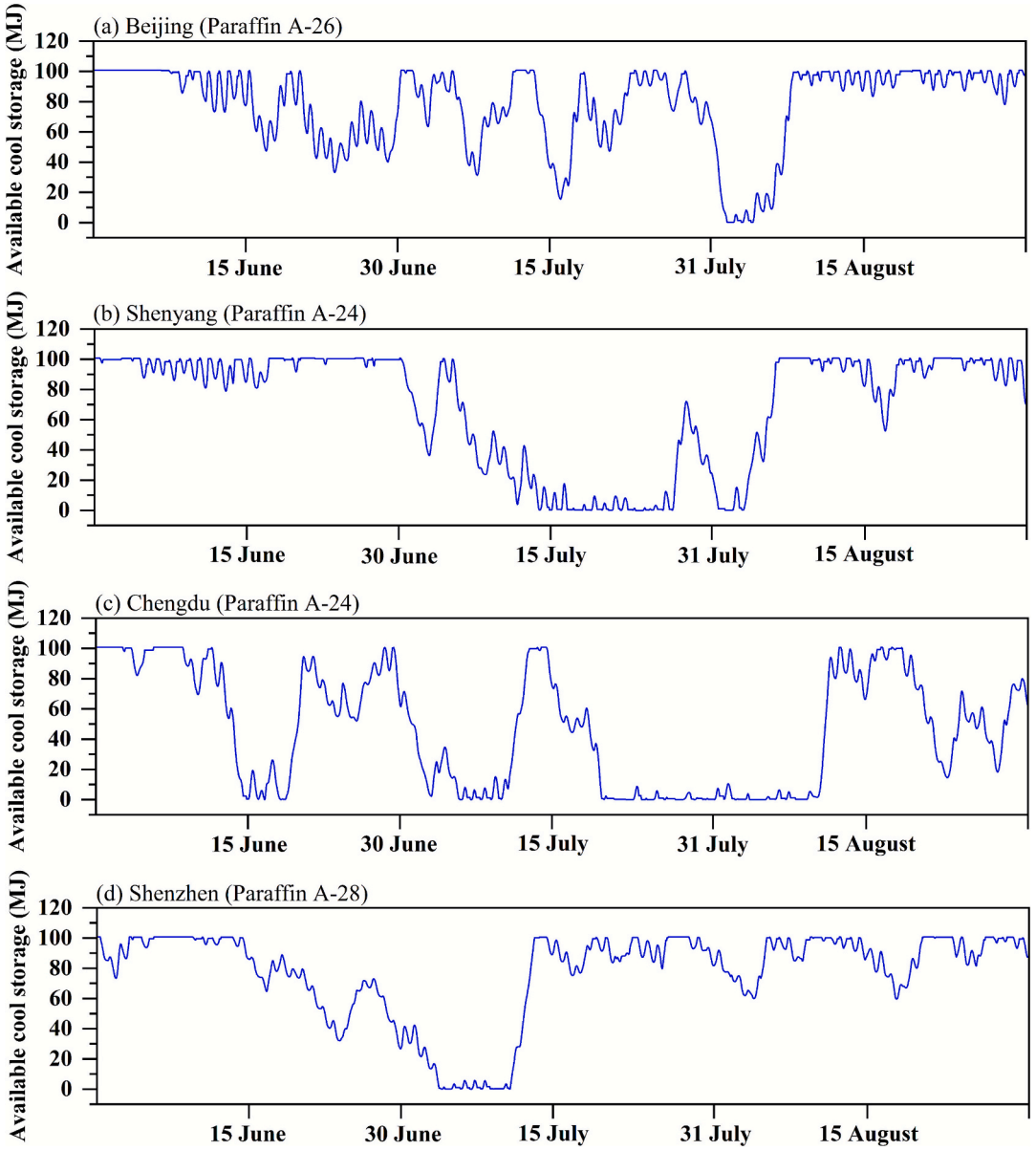

Fig. 8. Hourly available cool storage of the PCM-TES system across the summer months, shown for the optimal PCM type (maximum uptime). (a) Beijing. (b) Shenyang. (c) Chengdu. (d) Shenzhen.

Fig. 11. It was noteworthy that the electricity savings in Fig. 11 consisted of two parts: (1) the savings generated by preconditioning the OA with PCM in the new system, and (2) the savings resulting from increasing the ward set-point temperature from 24 ℃ to 28 ℃.

In Beijing, as the phase change temperature increased from 18 ℃ to 26 ℃, the electricity savings of the new system gradually rose from 2550 kWh to 2666 kWh. However, when the phase change temperature further increased to 28 ℃ and 30 ℃, the electricity savings decreased to 2598 kWh and 2561 kWh, respectively. Selecting the optimal PCM based on maximum electricity savings would correspond to a phase change temperature of 26 ℃, with an associated electricity saving rate of 68 %. This phase change temperature aligned with the one that yielded the maximum uptime percentage in Fig. 6.

In Shenyang, as the phase change temperature increased from 18 ℃ to 20 ℃ and 22 ℃, the electricity savings of the new system increased from 2757 kWh to 2807 kWh and 2875 kWh, respectively. With further increases in the phase change temperature, the electricity savings gradually declined. When the phase change temperature reached 30 ℃, the electricity savings had decreased to 2732 kWh. Similarly, the maximum electricity savings occurred at a phase change temperature of 22 ℃, corresponding to an electricity saving rate of 75 %. However, this differed from the phase change temperature associated with the maximum uptime percentage (24 ℃, refer to Fig. 6 (b)).

For Chengdu, as the phase change temperature increased from 18 ℃ to 24 ℃, the electricity savings gradually increased from 2689 kWh to 2797 kWh. Further increases in the phase change temperature led to a gradual reduction in electricity savings. At a phase change temperature of 30 ℃, the electricity savings decreased to 2693 kWh, a value close to that at 18 ℃. Unlike Beijing and Shenyang, the maximum electricity savings in Chengdu occurred at a phase change temperature of 24 ℃, with an electricity saving rate of 74 %. This temperature was consistent with the phase change temperature that resulted in the maximum uptime percentage of the PCM-TES system.

In Shenzhen, it could be observed that the electricity savings remained unchanged at 2333 kWh for phase change temperatures of 18 ℃, 20 ℃, 22 ℃, and 24 ℃. When the phase change temperature increased to 28 ℃, the electricity savings rose to 2390 kWh. However, at a phase change temperature of 30 ℃, the electricity savings decreased to

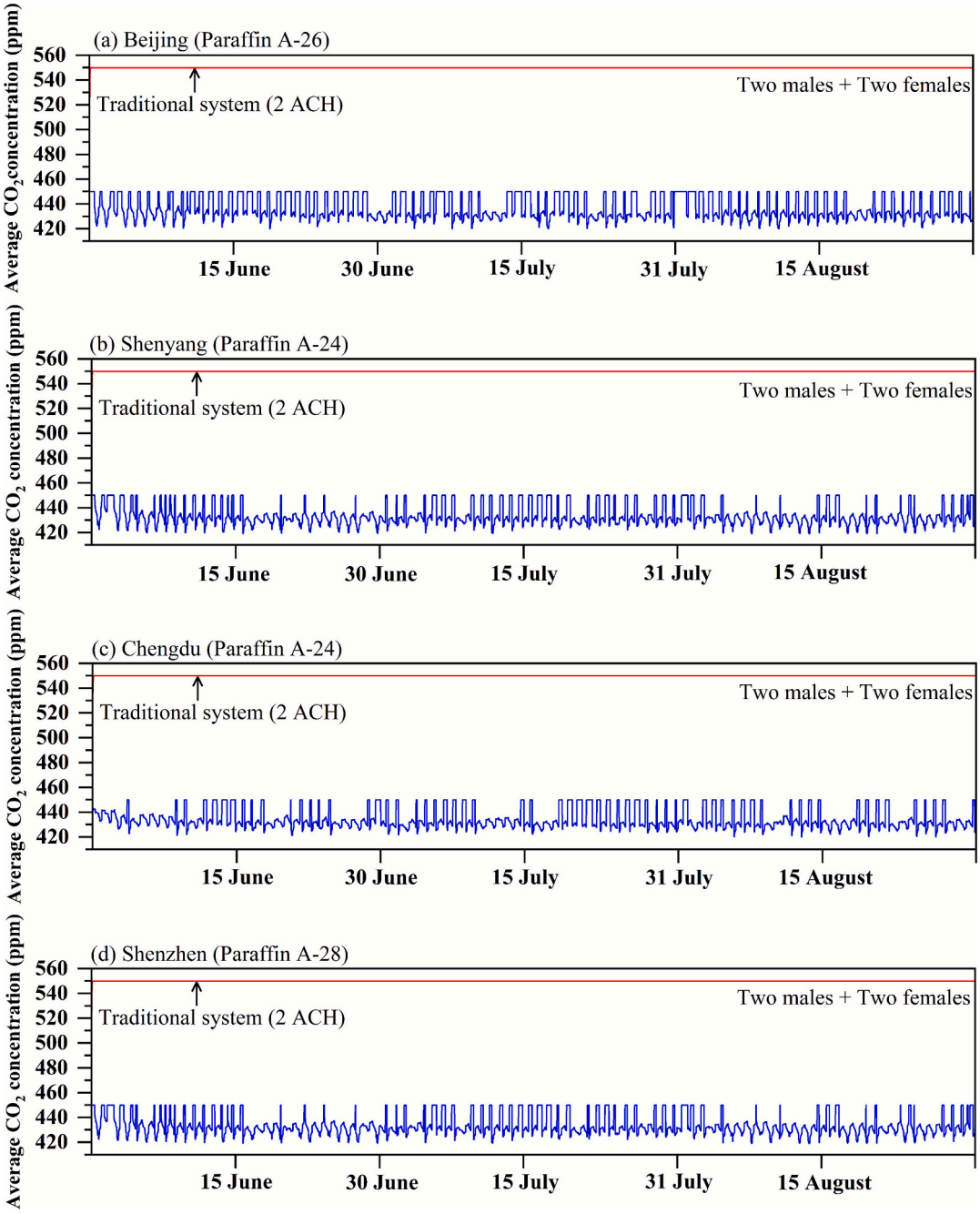

Fig. 9. Hourly evolution of the average CO_2 concentration in the four-person ward during the three summer months, shown for the optimal PCM type (maximum uptime). (a) Beijing. (b) Shenyang. (c) Chengdu. (d) Shenzhen.

2347 kWh. The phase change temperature corresponding to the maximum electricity savings was 28 ℃, which matched the temperature associated with the maximum uptime percentage of the PCM-TES system (refer to Fig. 6 (d)).

Overall, among the four cities, the new system achieved the highest electricity savings in Shenyang, followed by Chengdu, Beijing, and Shenzhen. The electricity savings in Shenzhen were significantly lower than those in the other three cities. Furthermore, the influence of the phase change temperature on electricity savings varied across cities. The maximum differences in electricity savings across different phase change temperatures were 116 kWh in Beijing, 143 kWh in Shenyang, 108 kWh in Chengdu, and 57 kWh in Shenzhen.

3.4. Sensitivity analysis

To enhance the robustness of the findings, a sensitivity analysis was conducted using Beijing (with a PCM phase-change temperature of 24 ℃ and an air supply temperature of 22 ℃) as a baseline case. The overall system performance was systematically examined under variations in the PCM phase-change temperature, the ward setpoint temperature, and the supply air temperature at the bed terminal. The corresponding uptime percentage of the PCM-air exchanger, the average ACH in the ward, and the total electricity savings under these different conditions are presented in Table 3.

When the fluctuation ranges of the PCM phase change temperature, ward setpoint temperature, and supply air temperature were 4 ℃ (±2 ℃), the corresponding fluctuations in the uptime percentage were 46 %,

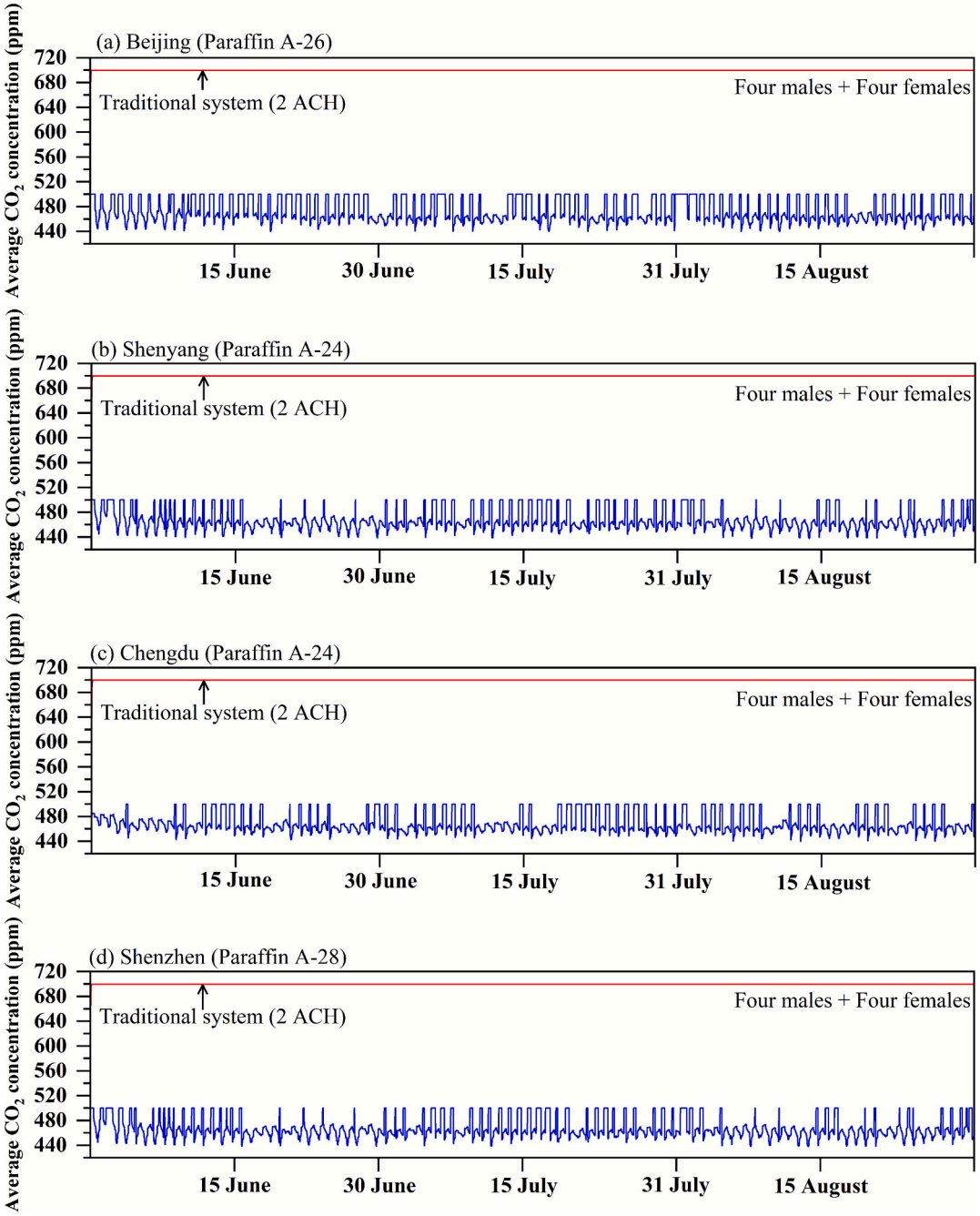

Fig. 10. Hourly evolution of the average CO_2 concentration in the eight-person ward during the three summer months, shown for the optimal PCM type (maximum uptime). (a) Beijing. (b) Shenyang. (c) Chengdu. (d) Shenzhen.

0 %, and 9 %, respectively. For the ward's average ACH during the three summer months, the corresponding fluctuation ranges were 0 $h^{-}1$, 3.0 $h^{-}1$, and 4.9 $h^{-}1$. Regarding electricity savings, the respective fluctuation amplitudes were 62 kWh, 2296 kWh, and 80 kWh. It was found that the factors exerting the greatest influence on the uptime percentage, average ACH, and electricity savings were the PCM phase-change temperature, supply air temperature, and room setpoint temperature, respectively.

4. Discussion

4.1. Overall performance of the newly proposed system

This study systematically investigated the operational performance of the PCM-TES system in the new system during summer, indoor air quality in the ward, and its energy-saving potential. These findings were of significant importance for a deeper understanding and broader application of the new system. The quantitative analysis of system performance provided essential baseline data and optimization targets for future system improvements. Meanwhile, the elevated ward set-point temperature of 28 ℃, while instrumental for energy conservation, was considered compatible with thermal comfort due to the concurrent use of the personalized bed terminal. This was qualitatively supported by findings from a prior human subject study [26], which indicated that with personalized control of the bed environment, thermal comfort could be maintained at ambient temperatures up to 28 ℃ for individuals lying in bed. Therefore, the 28 ℃ set-point was not solely an energy-saving measure but a feasible design parameter underpinned

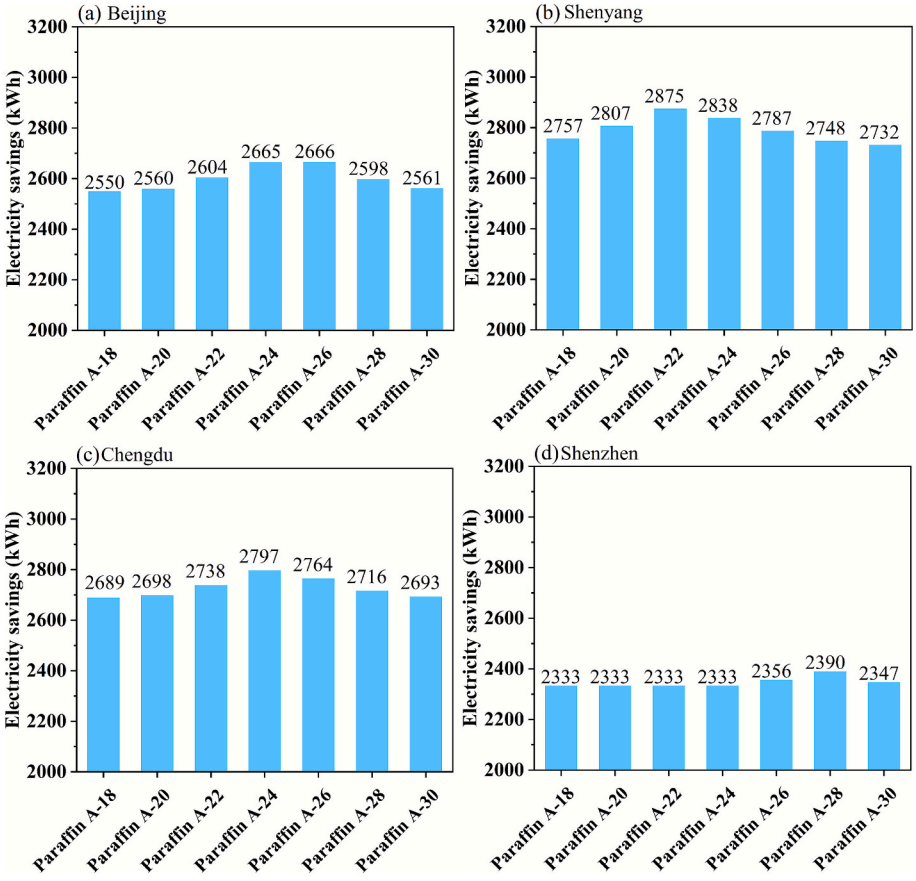

Fig. 11. Electricity savings of the newly developed system under different phase change temperatures across the three summer months. (a) Beijing. (b) Shenyang. (c) Chengdu. (d) Shenzhen.

Table 3
Performance of the system under various conditions.

Conditions	Uptime percentage (%)	Average ACH (h^{-1})	Electricity savings (kWh)
Baseline	63	8.7	2665
PCM – 22 ℃	29	8.7	2604
PCM – 26 ℃	75	8.7	2666
Setpoint temperature – 26 ℃	63	10.4	1599
Setpoint temperature – 30 ℃	63	7.4	3895
Air supply temperature – 20 ℃	54	7.0	2585
Air supply temperature – 24 ℃	63	11.9	2637

by the principle of personalized comfort, wherein the local cooling effect decoupled the occupant's thermal comfort from the elevated background temperature.

However, it was important to note that the numerical results presented, such as electricity savings and ACH values, were deterministic outcomes of the simulation under the specific assumptions defined in Section 2.5. While they provided a precise basis for comparison, their absolute precision needed to be interpreted with the understanding that real-world performance would be influenced by uncertainties in inputs such as the fixed EER, internal load profiles, and climate data.

Regarding the operational performance of the PCM-TES system, the selection of PCM was found to significantly influence its uptime percentage during summer. In all four cities investigated, by optimizing the phase change temperature, the PCM-TES system remained operational for over 60 % of the time (Fig. 6). This was because the relationship between the phase change temperature and OA temperature directly determined whether the PCM-TES system was activated or deactivated – a phenomenon well-documented in previous studies [53,54].

The hourly on/off status of the PCM-TES system offered further insight into its operational behavior. As shown in Fig. 7, the system remained active for noticeably longer periods than it was inactive across all four cities, which was consistent with the results in Fig. 6. The active state of the system included two scenarios: (1) the PCM-TES system was in discharging mode and still had available cool storage, or (2) it was in charging mode and had not yet reached full storage capacity. The opposite conditions corresponded to the system being deactivated. For example, in early June in Beijing (Fig. 7 (a)), the system remained off for an extended period because the outdoor temperature was consistently below the phase change temperature, and the system's cool storage was already full. Between June 25 and the end of July, the system operated continuously due to its ability to maintain repeated "discharging–charging" cycles.

Regarding the available cool storage, results indicated that under the current design, all four cities experienced periods when the available cool storage dropped to 0 MJ (Fig. 8). This occurred when outdoor temperatures remain consistently above the phase change temperature both day and night, leading to rapid consumption of stored cooling without effective completion of "discharging–charging" cycles, ultimately causing system failure. This was particularly notable in Shenyang and Chengdu. However, this issue could be mitigated by increasing the design capacity of the PCM-TES unit – that was, by using more PCM to enhance its latent heat storage capability. In practical engineering applications, however, a thorough evaluation was needed to

balance the initial investment and operational costs of adding more PCM against the resulting electricity savings. For example, Yun et al. [55] analyzed the economic feasibility of using PCM in buildings and found that economic benefits did not always increase monotonically with the amount of PCM. Therefore, a more detailed economic analysis should be conducted for the proposed system in future work.

In terms of improving indoor air quality, the new system significantly reduced average CO_2 concentrations compared to the conventional system. Even when occupant density was increased to 5 m^2/person, the average CO_2 concentration during the three summer months remained below 480 ppm in all four cities – a value only slightly higher than that of the OA. This was because the conventional system typically operated at a fixed ACH of 2 h^{-1}, whereas the new system had a minimum designed ACH of 6 h^{-1} (50 L/s per terminal). Meanwhile, the average ACH of the new system during the three months of summer reached about 4–5 times that of the traditional system. This indicated that the new system could effectively improve air quality throughout the entire ward. Our previous research confirmed the system's ability to ensure air quality in the patient's breathing zone [25], and this study provided a more comprehensive evaluation of its performance in improving whole ward air quality. The hourly fluctuations in CO_2 concentration (Figs. 9 and 10) resulted from variations in the system's operational status, which affected the total ACH supplied to the ward. Overall, however, due to the high minimum ACH of the new system and the relatively low CO_2 generation rate indoors, CO_2 concentrations fluctuated within a narrow range. This was consistent with pollutant dilution principles [51], wherein the amount of pollutant removed per unit of ventilation air decreased as the ventilation rate increased.

In terms of energy-saving potential, the new system demonstrated significant electricity savings across all four cities, with summer electricity savings exceeding 60 kWh/m^2. Savings in Shenzhen exhibited relatively lower electricity savings compared to the other three cities, mainly due to two factors: (1) the PCM-TES system had a shorter uptime percentage in Shenzhen, and (2) even when the system was running, the high outdoor temperatures were often close to the phase change temperature, which resulted in prolonged charging times and lower discharging efficiency. Although the energy-saving potential varied with different phase change temperatures, this variation was relatively small compared to the total electricity savings. This was because most of the electricity savings in the new system came from increasing the ward set-point temperature from 24 ℃ to 28 ℃, which was a core energy-saving strategy of PECS. The fundamental principle was that by maintaining personal comfort locally, a significantly higher and more energy-efficient background temperature could be tolerated. This decoupling of the background environment from occupant comfort was a key driver for energy reduction, as established in foundational PECS research [56] and reinforced in recent analyses [57]. Previous studies on conventional systems had shown that each 1 ℃ increase in the summer set-point temperature could reduce cooling energy consumption by approximately 10 %-20 % [58–60], a finding that our study extended to the novel context of a PCM-TES-OAS coupled with a bed-side PECS, thereby validating and aligning with the broader energy-saving trends reported in the literature. The electricity savings contributed by the PCM-TES system were also consistent with levels reported in earlier research [47].

Overall, the new system effectively increased the ventilation rate in the ward while significantly reducing energy consumption for environmental control. Moreover, since the micro-environment around the patient was individually controlled by the bed terminal, the new system demonstrated the ability to simultaneously ensure thermal comfort, respiratory health, and energy efficiency.

4.2. Practical retrofitting recommendations

This section elaborated on the differences between the new system and the conventional system from three aspects: (1) the installation of the bed terminal, (2) modifications to the air conditioning pipeline system, and (3) changes in unit selection. These aspects held significant engineering implications for both new construction and retrofitting of existing hospital wards.

Regarding the bed terminal, as shown in Fig. 12, it could be positioned at the head of the bed. This was consistent with our previous research on the bed micro-environment [25]. Moreover, due to its unique design, the terminal did not occupy much space and would not interfere with the normal activities of patients or medical staff. In addition, in actual ward settings, the head of the bed was usually placed against a side wall, which provided a convenient solution for routing the terminal's pipelines. The fresh air duct connected to the terminal could be installed along the wall, and the fresh air ducts from multiple bed terminals could be consolidated into a single duct running along the upper part of the room, which was then connected to the OAS. A flow control valve could be installed in the duct section near the bed terminal to regulate the air volume supplied to the terminal. Furthermore, similar to other PV systems [61], electric heating wires could be integrated inside the duct to allow patients to make secondary adjustments to the supply air temperature during actual operation.

In terms of the pipeline system, study results indicated that the ACH of fresh air reached 4–5 times that of the conventional system. If the same air supply velocity was to be maintained, the size of the fresh air duct must be adjusted accordingly. As for the indoor return air, its flow rate was reduced to 6–8 % of that in the conventional system, which necessitated a corresponding reduction in the size of the return air duct. Similarly, the size of the water pipelines should be adjusted based on the required cooling capacity. However, whether for air or water pipelines, hydraulic balancing must be recalibrated based on the conventional system.

For the OAS and FCU, reselection was required due to changes in the maximum cooling capacity demanded. The maximum cooling capacity required by the OAS and FCU under both the conventional and new systems is shown in Fig. 13. Overall, across the four cities studied, when the room was conditioned by the new system, the maximum cooling capacity of the OAS should be about three times that under the conventional system, while the maximum cooling capacity of the FCU should be approximately 0.3 times that under the conventional system.

5. Limitations and future works

Although this study conducted a comprehensive evaluation of the new system's performance, certain limitations remain. Firstly, the research only selected four typical cities from four climate zones as case studies. Subsequent work should include assessments across more climate zones and a wider range of cities. Secondly, the study exclusively

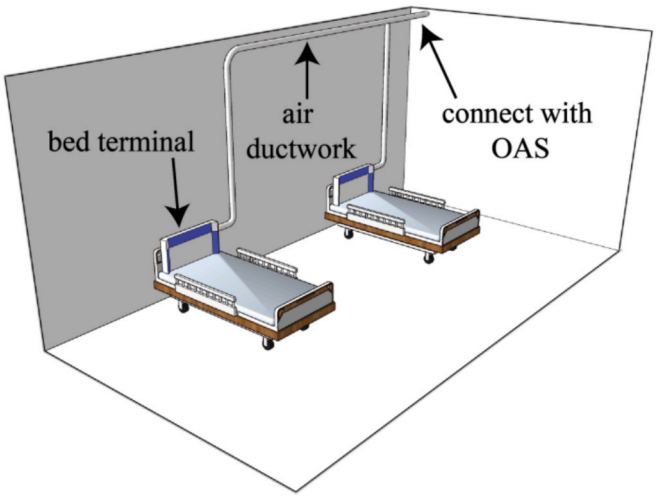

Fig. 12. Installation diagram for the hospital bed terminal.

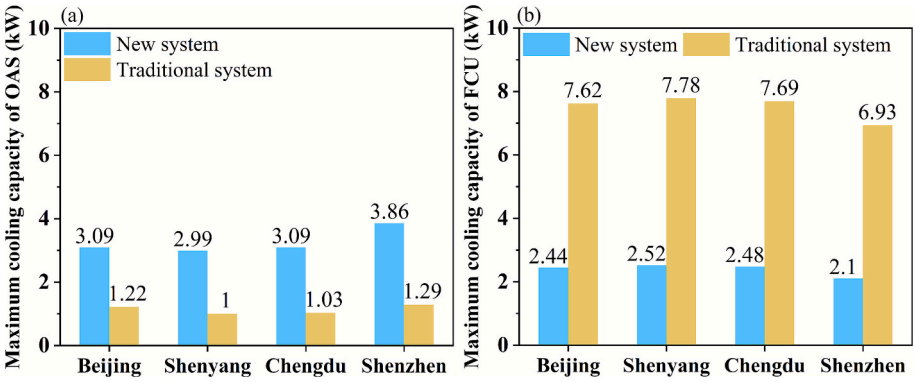

Fig. 13. The required maximum cooling capacity of the OAS and FCU.

employed plate-type PCM containers as the heat exchange units in the PCM-TES system. Given that the heat transfer performance of the PCM-TES system significantly influenced overall operation, future research should consider other types of PCM containers, such as tubular and shell-and-tube designs [62], as well as the impact of different PCM properties. Meanwhile, this study focused on a single ward and did not evaluate the system's performance across an entire medical building. As a result, the energy-saving potential analysis relied solely on the energy consumption of the units. Follow-up studies could expand the scope to include an actual medical building and further account for variations in energy consumption due to pipeline and fan operation. In addition, the numerical results presented in this study were deterministic outputs based on a specific set of input parameters and assumptions. The uncertainties inherent in these inputs (e.g., the performance of the PCM-air exchanger, the room set-point temperature, and the operating status of the bed terminal) could lead to deviations between the predicted and real-world system performance. Finally, an important limitation of this work was that the integrated PCM-TES-OAS system presented here had not yet undergone experimental or living-lab validation. The predictions for the system's operating status, IAQ, and energy savings, while based on theoretical analysis and simulations of the coupled system, were found to require empirical validation at the full-system level. The next steps involved a two-stage process: initial laboratory-scale validation of a full prototype in a controlled environmental chamber, followed by a field assessment in a pilot ward setting. These future controlled semi-real or field studies were crucial to verify the system-level operational robustness, actual thermal comfort performance, and IAQ outcomes in practice. This progression was essential for translating the conceptual framework into a practical technology.

6. Conclusions

This study presented a methodological framework for the PCM-TES-OAS system for creating personalized ward environments and conducted a comprehensive performance comparison with the traditional FCU + DOAS approach. Taking hospital wards in Beijing, Shenyang, Chengdu, and Shenzhen as examples, the summer operational performance of the PCM-TES system was investigated, along with indoor air quality and electricity savings when the ward was conditioned by the new system versus the conventional system. The main findings are as follows:

(1) The phase change temperature has a significant impact on the operational performance of the PCM-TES system. With an appropriately selected phase change temperature, the PCM-TES system can remain operational for over 60 % of the time in summer and achieve effective "charging-discharging" cycles of the PCM.
(2) When the ward is conditioned by the new system, the ACH can reach 8 h^{-1} to 10 h^{-1}, and the CO_2 concentration only fluctuates within a narrow range. Under these conditions, even when occupant density increases to 5 m^2/person, the average CO_2 concentration in the ward over the three summer months remains below 480 ppm. This indicates that the new system has the potential significantly improves indoor air quality.
(3) Across all four cities, the electricity savings estimated for the new system over the three summer months are no less than 60 kWh/m^2. This demonstrates that the new system shows substantial theoretical energy-saving potential while ensuring thermal comfort and considerably increasing the ACH.
(4) The required maximum cooling capacity of the OAS and FCU is found to be about 3 times and 0.3 times that of the conventional system, respectively. In addition, the hydraulic balance of the air conditioning pipeline system should be recalibrated.

CRediT authorship contribution statement

Wei Su: Writing – original draft, Visualization, Validation, Software, Methodology, Investigation, Formal analysis, Data curation. **Zhengtao Ai:** Writing – review & editing, Supervision, Resources, Project administration, Funding acquisition, Conceptualization. **Bin Yang:** Writing – review & editing. **Tiantian Du:** Writing – review & editing. **Zhengxuan Liu:** Writing – review & editing.

Declaration of competing interest

The authors declare that they have no known competing financial interests or personal relationships that could have appeared to influence the work reported in this paper.

Acknowledgements

This study was supported by the Fundamental Research Funds for the Central Universities (No. 531118010378); and the National Natural Science Foundation of China (No. 52208106).

Data availability

Data will be made available on request.

References

[1] B.S. Alotaibi, S. Lo, E. Southwood, et al., Evaluating the suitability of standard thermal comfort approaches for hospital patients in air-conditioned environments in hot climates, Build. Environ. 169 (2020) 106561.
[2] B. Nourozi, A. Wierzbicka, R. Yao, et al., A systematic review of ventilation solutions for hospital wards: addressing cross-infection and patient safety, Build. Environ. 247 (2024) 110954.
[3] R. Ji, S. Qu, Investigation and evaluation of energy consumption performance for hospital buildings in China, Sustainability 11 (2019) 1724.

[4] V. De Giuli, R. Zecchin, L. Salmaso, et al., Measured and perceived indoor environmental quality: Padua Hospital case study, Build. Environ. 59 (2013) 211–226.

[5] H. Salonen, M. Lahtinen, S. Lappalainen, et al., Design approaches for promoting beneficial indoor environments in healthcare facilities: a review, Intell. Build. Int. 5 (2013) 26–50.

[6] Bivolarova M P, Melikov A K, Kokora M, et al., Novel bed integrated ventilation method for hospital patient rooms, in: Proceeding of ROOMVENT 2014, 13th SCANVAC International Conference on Air Distribution in Rooms, 2014, 49-56.

[7] W. Su, Z. Ai, B. Yang, A novel phase change material based personal environment control system for hospital wards, Journal of Building Engineering 95 (2024) 110207.

[8] Ministry of Housing Urban and Rural Development, Code for design of general hospital (GB51039-2014), China Architecture & Building Press, Beijing, China, 2014 (In Chinese).

[9] ASHRAE Standard 170, Ventilation of health care facilities, American Society of Heating, Refrigeration, and Air-conditioning Engineers, Inc., Atlanta, GA, 2013.

[10] M. Zhen, L. Zhang, X. She, et al., Study on thermal comfort of gynecological tumor patients in hospital ward area, Energ. Buildings 329 (2025) 115230.

[11] W. Su, B. Yang, A. Melikov, et al., Infection probability under different air distribution patterns, Build. Environ. 207 (2022) 108555.

[12] K. Bawaneh, F. Ghazi Nezami, M. Rasheduzzaman, et al., Energy consumption analysis and characterization of healthcare facilities in the United States, Energies 12 (2019) 3775.

[13] Z. Shi, H. Qian, X. Zheng, et al., Seasonal variation of window opening behaviors in two naturally ventilated hospital wards, Build. Environ. 130 (2018) 85–93.

[14] N.M.A. Rahman, L.C. Haw, A. Fazlizan, A literature review of naturally ventilated public hospital wards in tropical climate countries for thermal comfort and energy saving improvements, Energies 14 (2021) 435.

[15] S. Park, Y. Choi, D. Song, et al., Natural ventilation strategy and related issues to prevent coronavirus disease 2019 (COVID-19) airborne transmission in a school building, Sci. Total Environ. 789 (2021) 147764.

[16] J. Liu, S. Zhu, M.K. Kim, et al., A review of CFD analysis methods for personalized ventilation (PV) in indoor built environments, Sustainability 11 (2019) 4166.

[17] S.M. Hooshmand, H. Zhang, H. Javidanfar, et al., A review of local radiant heating systems and their effects on thermal comfort and sensation, Energ. Buildings 296 (2023) 113331.

[18] D. Khovalyg, M.P. Bivolarova, J. Shinoda, et al., Personalized environmental control systems (PECS): systematic review of benefits for thermal comfort, air quality, health, and human performance, Build. Environ. 286 (2025) 113541.

[19] A.K. Melikov, B. Krejciríková, J. Kaczmarczyk, et al., Human response to local convective and radiant cooling in a warm environment, HVAC&R Research 19 (2013) 1023–1032.

[20] M.P. Bivolarova, A.K. Melikov, C. Mizutani, et al., Bed-integrated local exhaust ventilation system combined with local air cleaning for improved IAQ in hospital patient rooms, Build. Environ. 100 (2016) 10–18.

[21] Bivolarova M P, Melikov A K, Kokora M, et al., Performance assessment of a ventilated mattress for pollution control of the bed microenvironment in healthcare facilities, in: Proceeding of Healthy Buildings Europe 2015, 2015, 633.

[22] W. Su, Z. Ai, A.K. Melikov, Potential of a bed ventilation system in reducing the risk of exposure to contaminants in infectious wards, Journal of Building Engineering 84 (2024) 108525.

[23] G. Song, A.K. Melikov, G. Zhang, et al., Human response to the bed thermal environment generated by a ventilated mattress combined with local heating, Build. Environ. 241 (2023) 110461.

[24] D. Al-Assaad, I. Pigliautile, J. Shinoda, et al., Personalized environmental control systems (PECS): a systematic review of performance evaluation methods for thermal comfort, air quality and energy, Build. Environ. 284 (2025) 113471.

[25] W. Su, Z. Ai, B. Yang, A new personalized environment control system for hospital beds with design optimization by Taguchi-based grey relational analysis, Build. Environ. 267 (2025) 112206.

[26] W. Su, Z. Ai, A. Lipczynska, et al., An experimental investigation on the application potential of personal environmental control systems in hospital wards, Build. Environ. 114006 (2025).

[27] M.M. Sarafraz, M.R. Safaei, A.S. Leon, et al., Experimental investigation on thermal performance of a PV/T-PCM (photovoltaic/thermal) system cooling with a PCM and nanofluid, Energies 12 (2019) 2572.

[28] T. Ma, Z. Li, J. Zhao, Photovoltaic panel integrated with phase change materials (PV-PCM): technology overview and materials selection, Renew. Sustain. Energy Rev. 116 (2019) 109406.

[29] A. de Gracia, Dynamic building envelope with PCM for cooling purposes - Proof of concept, Appl. Energy 235 (2019) 1245–1253.

[30] B. Alshuraiaan, Efficient utilization of PCM in building envelope in a hot environment condition, International Journal of Thermofluids 16 (2022) 100205.

[31] P.K.S. Rathore, S.K. Shukla, An experimental evaluation of thermal behavior of the building envelope using macroencapsulated PCM for energy savings, Renew. Energy 149 (2020) 1300–1313.

[32] U. Masood, M. Haggag, A. Hassan, et al., Evaluation of phase change materials for pre-cooling of supply air into air conditioning systems in extremely hot climates, Buildings 14 (2023) 95.

[33] P.C. Singh, P. Halder, Performance assessment of an air-conditioning system utilizing a PCM-based annulus cylindrical latent heat storage, Arab. J. Sci. Eng. 49 (2024) 1759–1770.

[34] A.S. Soliman, M.S. Fouda, P. Cheng, Power saving in a central air conditioning system by using multiple PCMs integrated with fresh air path, Energ. Buildings 300 (2023) 113691.

[35] S. Takeda, K. Nagano, T. Mochida, et al., Development of a ventilation system utilizing thermal energy storage for granules containing phase change material, Sol. Energy 77 (2004) 329–338.

[36] D. Palanisamy, B.K. Ayalur, Development and testing of condensate assisted pre-cooling unit for improved indoor air quality in a computer laboratory, Build. Environ. 163 (2019) 106321.

[37] F. Herbinger, M. Bhouri, D. Groulx, Investigation of heat transfer inside a PCM-air heat exchanger: a numerical parametric study, Heat Mass Transf. 54 (2018) 2433–2442.

[38] B.E. Kareem, A.M. Adham, B.N. Yaqob, Design and optimization of air to PCM heat exchanger using CFD, Arab. J. Sci. Eng. 48 (2023) 12609–12623.

[39] T. Kamidollayev, J.P. Trelles, J. Thakkar, et al., Parametric study of panel PCM-Air heat exchanger designs, Energies 15 (2022) 5552.

[40] W. Su, Z. Ai, B. Yang, Performance of latent heat storage exchangers: Evaluation framework and fast prediction model, Renew. Energy 237 (2024) 121896.

[41] A. Garg, G. Singhal, Mathematical modeling for transient thermal performance analysis of phase change material-based heat exchanger, Appl. Therm. Eng. 216 (2022) 119029.

[42] L. Wang, J. Xia, Simulation of air flow field and temperature distribution in the ward of a newly-built hospital of post-COVID-19, Int. J. Nanosci. 23 (2024) 2350080.

[43] Ministry of Housing Urban and Rural Development, Design standard for energy efficiency of public buildings (GB50189-2015), China Architecture & Building Press, Beijing, China, 2015 (In Chinese).

[44] H. Kim, J. Oh, J. Hong, et al., Design optimization of finned multi-tube PCM heat exchanger for enhancing EV energy performance, Appl. Therm. Eng. 257 (2024) 124477.

[45] A.A.R. Darzi, S.M. Mousavi, M. Razbin, et al., Utilizing neural networks and genetic algorithms in AI-assisted CFD for optimizing PCM-based thermal energy storage units with extended surfaces, Therm. Sci. Eng. Prog. 54 (2024) 102795.

[46] F. Agyenim, N. Hewitt, P. Eames, et al., A review of materials, heat transfer and phase change problem formulation for latent heat thermal energy storage systems (LHTESS), Renew. Sustain. Energy Rev. 14 (2010) 615–628.

[47] X. Chen, Q. Zhang, Z.J. Zhai, Energy saving potential of a ventilation system with a latent heat thermal energy storage unit under different climatic conditions, Energ. Buildings 118 (2016) 339–349.

[48] A. Waqas, S. Kumar, Thermal performance of latent heat storage for free cooling of buildings in a dry and hot climate: an experimental study, Energ. Buildings 43 (2011) 2621–2630.

[49] S. Taheri, A. Razban, Learning-based CO_2 concentration prediction: Application to indoor air quality control using demand-controlled ventilation, Build. Environ. 205 (2021) 108164.

[50] M. Qi, X. Li, L.B. Weschler, et al., CO_2 generation rate in chinese people, Indoor Air 24 (2014) 559–566.

[51] W. Su, Z. Ai, J. Liu, et al., Maintaining an acceptable indoor air quality of spaces by intentional natural ventilation or intermittent mechanical ventilation with minimum energy use, Appl. Energy 348 (2023) 121504.

[52] A. De Gracia, L. Navarro, A. Castell, et al., Energy performance of a ventilated double skin facade with PCM under different climates, Energ. Buildings 91 (2015) 37–42.

[53] S.A. Nada, W.G. Alshaer, R.M. Saleh, Experimental investigation of PCM transient performance in free cooling of the fresh air of air conditioning systems, Journal of Building Engineering 29 (2020) 101153.

[54] Q. Zhang, T.A.S. Sazon, F.S. Fadnes, et al., Design optimization of the cooling systems with PCM-to-air heat exchanger for the energy saving of the residential buildings, Energy Convers. Manage.: X 23 (2024) 100630.

[55] B.Y. Yun, J.H. Park, S. Yang, et al., Integrated analysis of the energy and economic efficiency of PCM as an indoor decoration element: Application to an apartment building, Sol. Energy 196 (2020) 437–447.

[56] T. Hoyt, E. Arens, H. Zhang, Extending air temperature setpoints: simulated electricity savings and design considerations for new and retrofit buildings, Build. Environ. 88 (2015) 89–96.

[57] R. Rugani, M. Picco, D. Khovalyg, et al., Personalised environmental control systems (PECS) usage thresholds: a dynamic simulation approach to assess energy, cost, and emissions saving, Energy Built Environ. (2025).

[58] C. Sunardi, Y.P. Hikmat, A.S. Margana, et al., Effect of room temperature set points on energy consumption in a residential air conditioning, in, Proceeding of AIP Conference 2248 (2020) 070001.

[59] Z. Lin, C.K. Lee, S. Fong, et al., Comparison of annual energy performances with different ventilation methods for cooling, Energ. Buildings 43 (2011) 130–136.

[60] C.K. Lee, K.F. Fong, Z. Lin, et al., Year-round energy saving potential of stratum ventilated classrooms with temperature and humidity control, HVAC&R Research 19 (2013) 986–991.

[61] Z.D. Bolashikov, A. Melikov, M. Krenek, Improved performance of personalized ventilation by control of the convection flow around occupant body, ASHRAE Trans. 115 (2009).

[62] M. Iten, S. Liu, A. Shukla, A review on the air-PCM-TES application for free cooling and heating in the buildings, Renew. Sustain. Energy Rev. 61 (2016) 175–186.